

**Control of plasmon dynamics in coupled plasmonic hybrid mode microcavities**N. D. Lanzillotti-Kimura,<sup>1</sup> T. Zentgraf,<sup>1,2</sup> and X. Zhang<sup>1,3,\*</sup><sup>1</sup>*Nanoscale Science and Engineering Center, 3112 Etcheverry Hall, University of California, Berkeley, California 94720-1740, USA*<sup>2</sup>*Department of Physics, University of Paderborn, Warburger Straße 100, D-33098 Paderborn, Germany*<sup>3</sup>*Materials Sciences Division, Lawrence Berkeley National Laboratory, 1 Cyclotron Road, Berkeley, California 94720, USA*

(Received 28 March 2012; revised manuscript received 21 May 2012; published 10 July 2012)

Hybrid plasmonic microcavities display localized electromagnetic states similar to the confined electronic levels in atoms and quantum wells. Exploiting this parallelism and concepts used in photonics, we describe a novel plasmonic device based on the coupling between a plasmonic microcavity and a photonic microcavity. We theoretically analyze the coupling effects and the plasmon dynamics in structures integrated in silicon optical waveguides. We observe a strong coupling behavior between the eigenmodes that leads to a periodic excitation of the plasmonic hybrid mode in analogy to a plasmonic pulsar. We demonstrate that the spectra—and thus the dynamics—of confined plasmons can be tailored with great versatility in plasmonic pulsars in the 100-fs scale. These structures open new ways in the design and conception of plasmonic and photonic applications and the control and manipulation of hybrid plasmons in the time domain.

DOI: [10.1103/PhysRevB.86.045309](https://doi.org/10.1103/PhysRevB.86.045309)

PACS number(s): 73.20.Mf, 42.70.Qs, 78.67.Pt

**I. INTRODUCTION**

The dynamics of two-level systems have attracted the attention of researchers from diverse fields ranging from chemistry and solid state physics to photonics and nanophononics.<sup>1–5</sup> Perhaps one of the simplest two-level systems is a hydrogen molecule with two identical hydrogen atoms showing two hybridized energy levels. In spite of the simplicity of two-level systems, they have become extremely important for quantum optics, nuclear magnetic resonances, and quantum computation. Based on the two-level concept, photonic and nanophononic molecules have been previously proposed and also experimentally studied by concatenating two identical resonators.<sup>4,5</sup>

Another fascinating example of two-level systems is the exciton-polaritons: pseudoparticles that result from the strong coupling between excitons and photons can show properties of light or matter depending on the instantaneous measuring time.<sup>6</sup> The study of exciton-polariton enhanced Raman scattering, the polariton laser, and the polariton Bose–Einstein condensates are just a few of the recent striking results in this research direction.<sup>7–13</sup> The study of two-level systems capable of supporting hybrid pseudo particles, multiple spatial localizations, or even for storing energy remains an active and fundamental research topic in physics. Here, we analyze the time evolution of a system that is capable of supporting hybrid plasmonic and purely photonic states simultaneously. Hybrid plasmonic waveguides and hybrid plasmonic cavities have been previously introduced as an efficient way to achieve subwavelength light confinement and management.<sup>14,15</sup> Based on the concept of plasmonic hybrid modes a plasmonic nanoscale laser was even demonstrated.<sup>16</sup> In this work we analyze the eigenmode dynamics in a system where an optical microcavity is coupled to a hybrid plasmonic microcavity. We observe a strong coupling behavior between the eigenmodes that leads to a periodic excitation of the plasmonic hybrid mode cavity in analogy to a plasmonic pulsar.

Plasmonics has emerged as a promising field in physics, with the potential to overcome the diffraction limit in classical

photonics and to develop a myriad of applications. While surface plasmon polaritons allow the transmission of optical signals in a deep-subwavelength regime, spatially localized surface plasmons show strong electronic resonances that allow their use for the design of optical nanoantennas and metamaterials, among others.<sup>17</sup> The interaction between two or more plasmonic particles<sup>3</sup> gives rise to a hybridization of the plasmonic modes in analogy to the energy level hybridization in molecules, which can be used to tune the resonance frequency of the system. By engineering the electromagnetic resonances, the development of plasmonic metamaterials with negative index of refraction opened a new perspective towards achieving ultimate control of light in nanoscaled dimensions. With a few exceptions<sup>18</sup> the control of the plasmonic properties of these systems has been done only in the spectral domain, without any particular efforts devoted to the time domain dynamics. Examples for the spectral shaping include pure plasmonic molecules formed by the coupling of identical localized surface plasmonic modes, plasmon-induced transparency structures,<sup>3,19,20</sup> coupled split-ring resonators,<sup>21</sup> and metallic photonic crystals.<sup>22,23</sup>

In this paper we focus our attention on a silicon-based plasmonic pulsar; essentially, we address the time domain manipulation of a confined hybrid plasmon mode in the 10–500 fs timescale when coupled to a purely optical cavity mode. Our analysis shows that due to the excitation of the two eigenmodes in the coupled system the energy oscillates between the photonic and plasmonic resonators, showing a pulsing behavior in the hybrid plasmon cavity: the plasmonic pulsar. Furthermore, we analyze the geometrical parameters of this structure that determine the lifetime and beating period of the oscillation. The paper is organized as follows: Sec. II introduces the design and main characteristics of hybrid plasmonic–photonic microcavities (HPPM) and plasmonic molecules; the concept of plasmonic pulsars based on HPPM is discussed in Sec. III. Finally, the conclusions and future perspectives are presented in Sec. IV.

## II. HYBRID PLASMONIC-PHOTONIC MICROCAVITY

A Fabry-Perot resonator consists of two parallel highly reflective mirrors. The resonance condition is achieved whenever the separation of the mirrors matches an integer number of half-wavelengths. This resonance condition is characterized by an optimal transmission and an amplification of the electric field inside the resonator. Optical microcavities in silicon (Si) photonic waveguides are the equivalent of Fabry-Perot resonators, where the mirrors are replaced by distributed Bragg reflectors (DBRs). In the case studied in this work, the DBRs are formed by surface gratings consisting of a series of periodic grooves in a Si-based slab waveguide. For an optical mode propagating within the slab waveguide the DBRs lead to a characteristic photonic bandgap. Whenever the separation between the DBRs equals an integer number of effective half-wavelengths, a photonic confined mode will appear in the center of the bandgap. The underlying physics is the same described in the design of monolithic semiconductor optical microcavities and planar acoustic nanocavities.<sup>5,24,25</sup> Similar structures have been studied in the last decades to develop optoelectronic modulators and to study novel physical phenomena in photonic crystal fibers.<sup>26–29</sup>

Our proposed design is based on a standard 340-nm-thick Si waveguide on top of a thick SiO<sub>2</sub> layer. Such geometry can be achieved by using commercial Silicon-On-Insulator substrates. A scheme of the structure is shown in Fig. 1(a). On top of the Si slab waveguide two surface gratings play the role of DBRs, whereas the shape, size, and period of the grooves determine the optical stopband for a wave propagating inside the waveguide. The separation of the two DBRs will determine the spectral position of the confined optical mode within the formed cavity. For our analysis of a single hybrid plasmonic cavity we used 20 period DBRs separated by a (3λ) layer. Each grating period has a rectangular cross-sectional profile with 141 nm Si and 90 nm air, whereas the grooves have a depth of 90 nm.

For the system under investigation we replaced the confined optical cavity mode with a plasmonic hybrid mode. Such a HPPM is characterized by confining surface plasmon polaritons both spatially and spectrally. The plasmonic hybrid mode is formed by the hybridization of a surface plasmon with an optical waveguide mode, as proposed by Oulton *et al.*<sup>14</sup> Here we use a silver metal slab that is spatially separated by a thin film of a low-index insulator (SiO<sub>2</sub>) from the optical waveguide. Due to the coupling between the plasmon and waveguide mode a strongly confined hybrid plasmon mode is formed in the low-index insulator gap. Previous works have theoretically proposed cavities for hybrid plasmonic modes.<sup>30–33</sup> However, in these cases the integration with Si-compatible photonics was limited. Some concepts were based on a photonic crystal placed on top of an infinitely extended metallic surface.<sup>30,32</sup> The drawback of such an approach is the limitation of the dimensions of the systems to the characteristic propagation lengths of the hybrid plasmon modes. In addition, these structures do not allow a concatenation of plasmonic and optical microcavities in an evident way, as we will propose in the next section. Another approach to achieve a hybrid plasmonic cavity is the modification of a microdisk resonator.<sup>31,33</sup> In this case the optimization of the input and

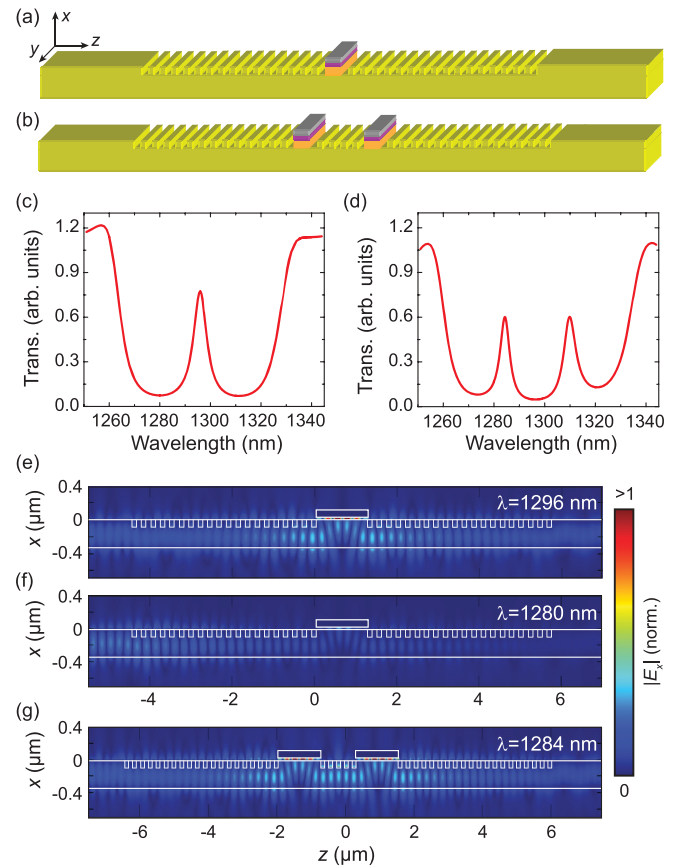


FIG. 1. (Color online) Hybrid plasmonic structures based on optical microcavities. (a) Scheme of a plasmonic microcavity: the structure is formed by two gratings acting as DBRs enclosing an optical spacer; on top of the optical spacer an Ag layer separated by a SiO<sub>2</sub> thin film generates the localized plasmonic-photonic mode. (b) Scheme of a plasmonic molecule formed by two concatenated plasmonic microcavities. (c) and (d) Calculated optical transmission for the single plasmonic and plasmonic molecule structure, respectively. (e) Calculated norm of the electric field component  $E_x$  for an incident wavelength  $\lambda = 1296$  nm for the single plasmonic microcavity. (f) Same as (e) but for the stopband wavelength  $\lambda = 1280$  nm where no transmission occurs. (g) Calculated norm electric field component  $E_x$  for a wavelength  $\lambda = 1284$  nm in the plasmonic molecule structure with two coupled cavities (see Supplemental Material<sup>34</sup>).

output coupling of the modes from and to a photonic circuit increases the complexity of the system; the  $Q$  factor cannot be controlled easily by design. In order to create the HPPM we added in the cavity region between the two surface gratings a 100-nm-thick Ag film only on top of the Si waveguide layer, separated by a 20-nm-thick SiO<sub>2</sub> film. The thickness of the SiO<sub>2</sub> determines the electric field confinement in the vertical ( $x$ ) direction. The structural parameters were chosen to optimize the cavity performance around 1295 nm; for the sake of simplicity we will not analyze here the dependence on the grating parameters of the DBRs. By placing the metallic film *only* on top of the waveguide in between the DBRs, the optical losses associated with the metal are limited to this region and thus resulting in a reduced loss when compared with other plasmonic cavities where the metallic losses are distributed through the entire structure.

For the transmission of an optical waveguide mode through our designed HPPM structure [as shown in Fig. 1(a)] we obtain a characteristic stop band due to the DBRs [Fig. 1(c)]. All simulations have been performed using the commercial software package COMSOL Multiphysics assuming a 2D geometry. The formed minigap for the structure is well defined between 1265 and 1330 nm. The transmission peak at 1296 nm corresponds to the confined mode in the HPPM. This cavity mode has a full width at half maximum (FWHM) of 6.2 nm and a maximum transmission of 55%. The FWHM can be controlled by the number of periods in the external DBRs. We note that the transmission of the mode in the minigap is limited by radiative losses due to scattering at the gratings and absorption in the Ag layer. Figures 1(e) and 1(f) show the magnitude of the electric field distribution ( $|E_x|$ ) in the structure for waveguide mode with wavelengths  $\lambda = 1296$  nm and  $\lambda = 1280$  nm, respectively, travelling from left to right in positive  $z$  direction. For the confined cavity mode [Fig. 1(e)] the electric field is mainly located in the thin SiO<sub>2</sub> film underneath the metal, where it has a peak value 10 times higher than the field in the center of the corresponding bare Si waveguide (without the HPPM structure). In Fig. 1(f) (corresponding to the high reflectivity region in the bandgap) the waveguide mode is reflected by the DBRs, resulting in a vanishing field in the cavity and almost zero transmission (see Supplemental Material<sup>34</sup>).

In the following we extend the concept to two coupled cavities. Such a double plasmonic cavity is the equivalent of a “plasmonic molecule” and can be constructed by coupling the discrete energy states of two plasmonic resonators. Two concatenated cavities can be created in a single structure by using three DBRs separated by two homogenous waveguide regions in the same way as a photonic molecule can be designed [see Fig. 1(b)]. If the two plasmonic microcavities are identical, there is a splitting of the degenerate modes into a new set of modes that correspond to the complete system of coupled resonators. Figure 1(d) shows the calculated optical transmission for the two concatenated plasmonic microcavities. The coupling, i.e., the spectral separation of the modes, is determined by the reflectivity of the central DBR

whereas the lifetime of the modes is mainly determined by the reflectivity of the external DBRs and the length of the cavity. As an example the electric field distribution ( $|E_x|$ ) of one of the plasmonic molecule modes is plotted in Fig. 1(g) where it can be seen that the electric field is equally distributed between the two HPPMs, and it is enhanced in the thin SiO<sub>2</sub> gap layers.

In the next section we will analyze the coupling between an optical microcavity and a HPPM.

### III. PLASMONIC PULSARS

The structure shown in Fig. 1(b) supports an additional degree of freedom. If we consider the plasmonic molecule, it is possible to “transform” one of the two hybrid plasmonic microcavities into a pure photonic microcavity. In this case the structure couples a pure photonic state (optical microcavity mode) with a pure hybrid plasmonic state. This system features again two coupled eigenmodes and each of them has its energy distributed in the two resonators as in the case of the plasmonic molecule. We term this kind of coupled structure a plasmonic pulsar based on the dynamics in such a system, as it will be shown below. A scheme of a plasmonic pulsar structure, made of 20-period external DBRs, a five-period central DBR, and two  $3\lambda$  cavities, is displayed in Fig. 2(a). Here we consider an asymmetric structure consisting of two cavities—one photonic and one plasmonic—limited by identical mirrors at the left and right sides and connected to an optical Si slab waveguide on both sides. Again we can identify a low-transmission band between 1250 and 1350 nm, which is originated by the DBRs [Fig. 2(b)]. Two peaks at 1283 and 1312 nm correspond to the two eigenmodes of the plasmonic pulsar and appear symmetrically located with respect to the noncoupled mode energy [compare with Fig. 1(c)]. The dynamics of this system is described by the coupling of the two individual resonators. Hence, the spectra and dynamics of the double cavity structure are determined by the central DBR that defines the coupling strength between the two confined modes.

In Fig. 2(c) we show the calculated norm of the electric field in the  $x$  direction for an incident wavelength  $\lambda = 1283$  nm for the five periods’ central DBR structure, corresponding to

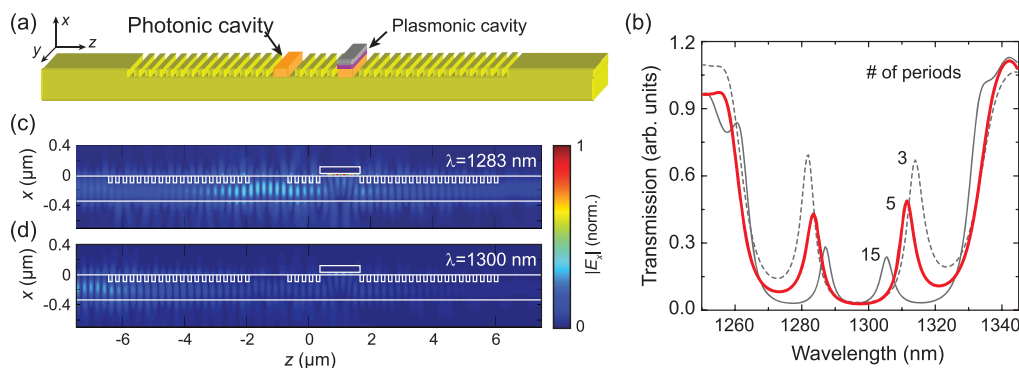


FIG. 2. (Color online) Hybrid plasmonic–photonic pulsar. (a) Scheme of the structure: the pulsar is formed by two gratings acting as external DBRs enclosing two optical spacers separated by a coupling central DBR; on top of the right optical spacer an Ag layer separated by a 20-nm-thick SiO<sub>2</sub> film generates the localized plasmonic–photonic mode. (b) Calculated optical transmission for the plasmonic pulsar structure for 3, 5, and 15 periods in the central DBR. The peaks for the five-period DBR at 1283 nm and 1312 nm correspond to the confined eigenmodes of the structure. (c) and (d) Calculated norm of the electric field in the  $x$  direction for an incident wavelength  $\lambda = 1283$  nm and 1300 nm, respectively, for the five periods’ central DBR structure (see Supplemental Material<sup>34</sup>).

one of the confined modes. For both eigenmodes the field is distributed between both cavities. In contrast Fig. 2(d) shows the case of  $\lambda = 1300$  nm where the field is mainly reflected resulting in a low transmission and weak fields inside the cavities (see Supplemental Material<sup>34</sup>).

In the plasmonic pulsar structure, one of the cavities confines a hybrid plasmon mode with the high field in the low index SiO<sub>2</sub> gap while the other one confines a purely optical waveguide mode. Since we have designed both modes to have the same eigenenergy before coupling, they will split into a symmetric and an antisymmetric mode, exactly in the same way it happens in the HPPM molecule. In the time domain, when both modes are excited in phase, the energy will oscillate between the two cavities, i.e., when the wave packet is localized in the right cavity of the structure, the energy is stored in the plasmonic hybrid mode; when the energy is localized in the left cavity of the structure, it is purely photonic.

If both eigenmodes of the plasmonic pulsar are simultaneously excited, the energy will periodically oscillate between the photonic and hybrid plasmon mode cavities with a characteristic oscillation time. This oscillation time can be controlled by modifying the coupling between the two structures. In Fig. 2(b) we also show the variation of the mode splitting and transmission of a pulsar structure for three different central DBR sizes. As it can be seen, the separation of the modes decreases as the number of periods in the central DBR increases. Smaller separations will result in longer oscillation times of the plasmonic pulsar. Note that for a large number of periods for the central DBR the system would behave as two decoupled cavities, and the dynamics is mainly controlled by the leakage through the external mirrors.

In the previous section it was shown that the coupling constant can be reduced by increasing the reflectivity of the central mirror and thus resulting in a reduced beating period between the modes. This behavior is in analogy to the hydrogen molecule or a purely phononic molecule where the energy can be transferred completely between the two identical ‘atoms’.

We can extend this analogy to the carbon monoxide (CO) molecule. This molecule combines two different atoms with similar electronic levels in a single molecule. Due to the coupling the energy levels hybridize and the coupled energy levels of the molecule differ from the original isolated atoms. Interestingly, if we extend the concept of the plasmonic CO molecule to the plasmonic pulsar structure, it is possible to obtain a constant energy stored in one of the cavities, e.g., the plasmonic cavity, in addition to the pulsing component between the two structures. The ratio between these two components can be tuned by changing either the size of the photonic cavity layer or the size of the plasmonic cavity structure; in such a way the cavities will become detuned. As a result the entire coupled structure becomes a pulsed source of plasmons where both the constant (DC) and periodic (AC) components can be controlled independently. As stated before, the AC component is fixed by the reflectivity of the central DBR, while the DC component is determined by the detuning between the two cavities. Figure 3(a) shows the effect of the mode coupling in the plasmonic pulsar on the spectral position of the new eigenmodes (and therefore the beating period) as a function of the detuning of the photonic optical cavity size for a constant central DBR size of five

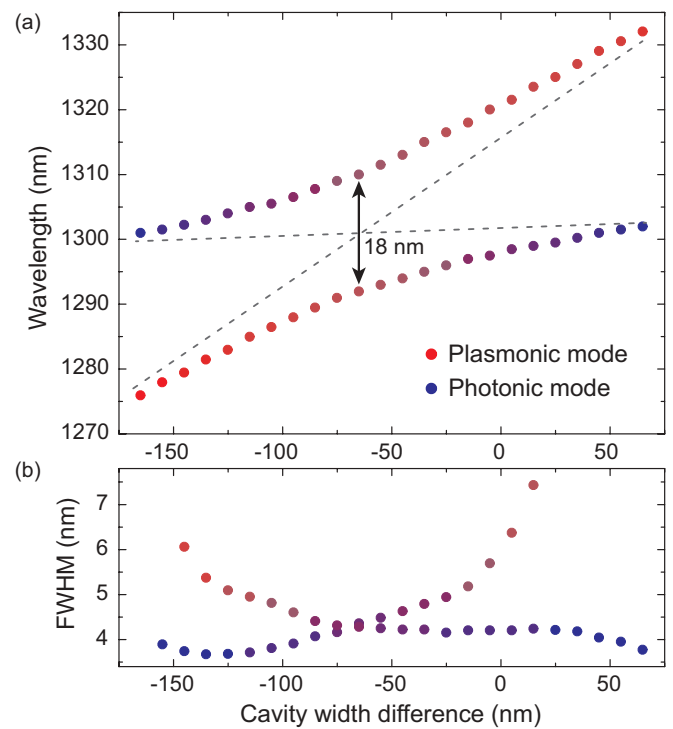


FIG. 3. (Color online) Coupling effects in the plasmonic pulsar. (a) Wavelengths of the plasmonic pulsar modes as a function of the detuning of the photonic optical microcavity size with respect to the plasmonic hybrid mode cavity size. The number of periods of the central (external) DBRs are kept constant to 7 (20) periods. The size of the plasmonic cavity is 1290 nm. The color coding (red/blue) indicates the dominant character of the mode (plasmonic/photonic). (b) Corresponding linewidths of the modes.

periods. Note that the minimum spectral separation between the modes, i.e., the strongest coupling, takes place when the optical cavity is  $\sim 65$  nm smaller than the plasmonic cavity. Red/gray (blue/black) color of the circles is a guide to the eye to indicate a plasmonic (photonic) character of the mode. When the optical cavity is strongly detuned from the plasmonic cavity the two modes are almost uncoupled; one of the modes is mainly localized in the left (photonic) cavity, while the other one is localized in the right (plasmonic) cavity. Under this condition an excitation of both modes will not produce the oscillatory behavior of the pulsar but only the DC component. Figure 3(a) shows the FWHM of the modes as a function of the optical cavity detuning with respect to the plasmonic cavity. It is important to note that, (i) the plasmoniclike modes have shorter lifetimes (larger FWHM) than the photoniclike ones; (ii) when the system is in the strong coupling condition both modes have the same FWHM; and (iii) the complex dependence of the FWHM with the detuning shows that other loss mechanism besides the absorption in the metal take place in the system, such as scattering at the gratings.

By comparing the plasmon dynamics of the plasmonic molecule with the plasmonic pulsar, one can observe that the systems behave in a quite similar way. Nevertheless two features deserve special attention. (i) The plasmonic pulsar is less lossy than the plasmonic molecule due to the absence of a second metallic cavity region and the coupling into the

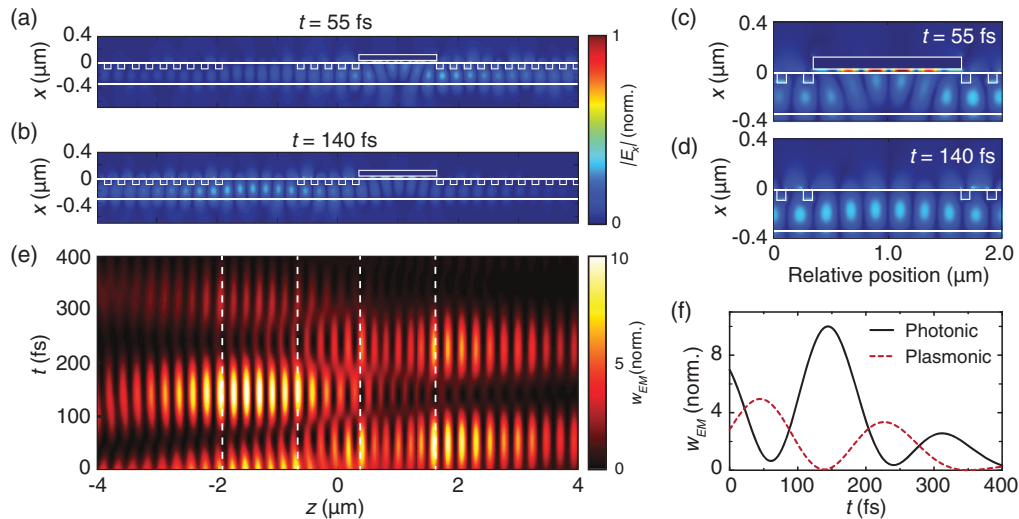


FIG. 4. (Color online) Simulated time evolution in a hybrid plasmonic pulsar when the two eigenmodes are excited simultaneously. (a) Electric field corresponding to the time at  $t = 55$  fs where the field is strongly localized in the right (plasmonic) cavity. (b) Same as (a) but for the time  $t = 140$  fs when the field is localized in the left (photonic) cavity. (c) and (d) Magnified view of the electric field  $|E_x|$  in the region of the hybrid plasmonic cavity for (a) and the photonic cavity for (b). (e) Time evolution of the total energy density in the structure integrated along the  $x$  axis. The vertical dashed lines indicate the position of the photonic and plasmonic cavities. (f) Black (solid) and red (dashed) curves show the oscillation of the total energy density at the center of the photonic and plasmonic cavity, respectively, as a function of time (see Supplemental Material<sup>34</sup>).

photonic crystal is almost lossless. Thus, the lifetime of the pulsar is longer than the lifetime of the plasmonic molecule. (ii) The second cavity (photonic) is part of the waveguide, so only the plasmonic cavity represents an external structure. This could be advantageous in the case that an active region is used for time sensitive sensing or to control time-dependent interactions.

In the previous sections we analyzed the spectral characteristics of the plasmonic cavities, molecules and pulsars. In the following we will analyze the time evolution of a plasmonic pulsar in more detail for the case that the two eigenmodes of the plasmonic pulsar are excited simultaneously.

The time evolution of an optical wavepacket (pulse) can be computed as

$$\varphi_k(x, z, t) = \frac{1}{2\pi} \int_{-\infty}^{\infty} \varphi_k(x, z, \omega) e^{-i\omega t} d\omega,$$

where  $\varphi_i$  is the electric or magnetic field component with  $k$  corresponding to the  $x$ ,  $y$ , and  $z$  components. Using the spatial field distributions calculated for a spectral band of 21 nm around each of the modes, we compute the time evolution when the plasmonic pulsar is excited. In Fig. 4 we show the resulting time evolution of the electric field component  $E_x$  in the structure. Panel (a) shows the electric field at a time  $t = 55$  fs, where we observe that it is mainly localized in the region of the plasmonic microcavity (right part of the structure). We define this state of the system as the hybrid plasmonic mode. On the contrary, on a time step of  $t = 140$  fs [panel (b)] the field is localized in the other half of the structure, i.e., in the photonic cavity (left part of the structure; see Supplemental Material<sup>34</sup>). Close-ups of both regions are shown in (c) and (d), respectively. Note the strong field localization in the thin SiO<sub>2</sub> layer between the metallic film and the Si waveguide for the plasmonic hybrid

mode cavity. It is a clear signature for the excitation of the surface plasmon mode on the metal surface at the time step of 55 fs. For a more intuitive picture of the time dynamics we plot the integrated energy density in the  $x$  direction over time in panel (e). The vertical dashed lines indicate the position of the photonic and plasmonic cavities along the  $z$  direction. One can clearly observe that the energy oscillates between the two cavities with an oscillation period of  $\sim 170$  fs. During this oscillation the energy density is reduced and finally fades away due to the cavity and absorption losses after 300 fs. The oscillation of the energy between the two cavities becomes more obvious in Fig. 4(f), where the integrated energy density is plotted for one point in the center of the photonic (black solid line) and plasmonic (red/dark gray dashed line) cavities. As mentioned previously, the oscillation time of 170 fs can be controlled by changing the number of periods in the central DBR, resulting in a different pulsation time for the hybrid plasmonic mode.

#### IV. CONCLUSIONS

We introduced the concept of a plasmonic pulsar, consisting of a photonic microcavity coupled to a hybrid plasmonic mode cavity. The engineering of the DBRs, cavity width, spacers, and materials can lead to highly optimized plasmonic cavity structures where not only the spatial localization can be manipulated but also the plasmonic time dynamics. The presented structure opens a new way in generating periodically excited surface plasmon polaritons from a purely photonic waveguide mode. We found that the pulsing period and lifetime of the plasmonic pulsar can be controlled by designing the photonic structure independently of the characteristics of the plasmonic microcavity. This characteristic opens the possibility of coupling photonic devices and plasmonic structures,

where the coupling strength is determined by the coupling DBR. Moreover, based on the same principle, the coupling mechanism could be potentially extended to other pseudo particles like phonons and polaritons, offering a new way to study new physical phenomena. The confinement characteristics could provide the platform to perform enhanced Raman scattering and nonlinear optical experiments in Si-compatible waveguides, the integration with plasmonic lasers, and the study of generalized coupled hybrid cavity systems.

## ACKNOWLEDGMENTS

This work is supported by the US Air Force Office of Scientific Research (AFOSR) MURI program (Grant No. 29017650-51649-B), the National Science Foundation Nano-scale Science and Engineering Center (NSF-NSEC) for Scalable and Integrated NAnoManufacturing (SINAM) (Grant No. CMMI-0751621), and the Deutsche Forschungsgemeinschaft (Grant No. ZE953/1-1).

\*Corresponding author: xzhang@me.berkeley.edu

- <sup>1</sup>C. Kittel, *Introduction to Solid State Physics*, 7th ed. (John Wiley & Sons, Inc., New York, 1996).
- <sup>2</sup>F. Y. Wu, S. Ezekiel, M. Ducloy, and B. R. Mollow, *Phys. Rev. Lett.* **38**, 1077 (1977).
- <sup>3</sup>S. Zhang, D. A. Genov, Y. Wang, M. Liu, and X. Zhang, *Phys. Rev. Lett.* **101**, 047401 (2008).
- <sup>4</sup>M. Bayer, T. Gutbrod, J. P. Reithmaier, A. Forchel, T. L. Reinecke, P. A. Knipp, A. A. Dremin, and V. D. Kulakovskii, *Phys. Rev. Lett.* **81**, 2582 (1998).
- <sup>5</sup>N. D. Lanzillotti-Kimura, A. Fainstein, C. A. Balseiro, and B. Jusserand, *Phys. Rev. B* **75**, 024301 (2007).
- <sup>6</sup>C. Weisbuch, M. Nishioka, A. Ishikawa, and Y. Arakawa, *Phys. Rev. Lett.* **69**, 3314 (1992).
- <sup>7</sup>D. Sanvitto, F. M. Marchetti, M. H. Szymańska, G. Tosi, M. Baudisch, F. P. Laussy, D. N. Krizhanovskii, M. S. Skolnick, L. Marrucci, A. Lemaître, J. Bloch, C. Tejedor, and L. Viña, *Nature Phys.* **6**, 527 (2010).
- <sup>8</sup>E. Wertz, L. Ferrier, D. D. Solnyshkov, R. Johne, D. Sanvitto, A. Lemaître, I. Sagnes, R. Grousson, A. V. Kavokin, P. Senellart, G. Malpuech, and J. Bloch, *Nature Phys.* **6**, 860 (2010).
- <sup>9</sup>G. Malpuech, A. Di Carlo, A. Kavokin, J. J. Baumberg, M. Zamfirescu, and P. Lugli, *Appl. Phys. Lett.* **81**, 412 (2002).
- <sup>10</sup>G. Malpuech, A. Kavokin, A. Di Carlo, and J. J. Baumberg, *Phys. Rev. B* **65**, 153310 (2002).
- <sup>11</sup>A. Fainstein, B. Jusserand, and V. Thierry-Mieg, *Phys. Rev. Lett.* **75**, 3764 (1995).
- <sup>12</sup>A. Fainstein, B. Jusserand, and V. Thierry-Mieg, *Phys. Rev. B* **53**, R13287 (1996).
- <sup>13</sup>A. Fainstein and B. Jusserand, *Phys. Rev. B* **57**, 2402 (1998).
- <sup>14</sup>R. F. Oulton, V. J. Sorger, D. A. Genov, D. F. P. Pile, and X. Zhang, *Nature Photon.* **2**, 496 (2008).
- <sup>15</sup>V. J. Sorger, Z. Ye, R. F. Oulton, Y. Wang, G. Bartal, X. Yin, and X. Zhang, *Nature Comm.* **2**, 331 (2011).
- <sup>16</sup>R. F. Oulton, V. J. Sorger, T. Zentgraf, R. M. Ma, C. Gladden, L. Dai, G. Bartal, and X. Zhang, *Nature* **461**, 629 (2009).
- <sup>17</sup>S. A. Maier, *Plasmonics: Fundamentals and Applications*, 1st ed. (Springer, New York, 2007).
- <sup>18</sup>T. Zentgraf, A. Christ, J. Kuhl, and H. Giessen, *Phys. Rev. Lett.* **93**, 243901 (2004).
- <sup>19</sup>N. Liu, L. Langguth, T. Weiss, J. Kästel, M. Fleischhauer, T. Pfau, and H. Giessen, *Nat. Mater.* **8**, 758 (2009).
- <sup>20</sup>R. D. Kekatpure, E. S. Barnard, W. Cai, and M. L. Brongersma, *Phys. Rev. Lett.* **104**, 243902 (2010).
- <sup>21</sup>R. Marques, F. Mesa, J. Martel, and F. Medina, *IEEE Trans. Antennas Propag.* **51**, 2572 (2003).
- <sup>22</sup>I. El-Kady, M. M. Sigalas, R. Biswas, K. M. Ho, and C. M. Soukoulis, *Phys. Rev. B* **62**, 15299 (2000).
- <sup>23</sup>J. T. Shen and P. M. Platzman, *Phys. Rev. B* **70**, 035101 (2004).
- <sup>24</sup>M. S. Skolnick, T. A. Fisher, and D. M. Whittaker, *Semicond. Sci. Technol.* **13**, 645 (1998).
- <sup>25</sup>N. D. Lanzillotti-Kimura, A. Fainstein, B. Perrin, B. Jusserand, A. Soukiasian, X. X. Xi, and D. G. Schlom, *Phys. Rev. Lett.* **104**, 187402 (2010).
- <sup>26</sup>P. R. Villeneuve, D. S. Abrams, S. Fan, and J. D. Joannopoulos, *Opt. Lett.* **21**, 2017 (1996).
- <sup>27</sup>M. Y. Liu and S. Y. Chou, *Appl. Phys. Lett.* **68**, 170 (1996).
- <sup>28</sup>S. Fan, J. D. Joannopoulos, J. N. Winn, A. Devenyi, J. C. Chen, and R. D. Meade, *J. Opt. Soc. Am. B* **12**, 1267 (1995).
- <sup>29</sup>G. Kakarantzas, T. A. Birks, and P. St. J. Russell, *Opt. Lett.* **27**, 1013 (2002).
- <sup>30</sup>X. D. Yang, A. Ishikawa, X. B. Yin, and X. Zhang, *ACS Nano* **5**, 2831 (2011).
- <sup>31</sup>B. Min, E. Ostby, V. Sorger, E. Ulin-Avila, L. Yang, X. Zhang, and K. Vahala, *Nature* **457**, 455 (2009).
- <sup>32</sup>M. Kim, S. H. Lee, M. Choi, B. H. Ahn, N. Park, Y. H. Lee, and B. Min, *Opt. Express* **18**, 11089 (2010).
- <sup>33</sup>Y.-F. Xiao, Y.-C. Liu, B.-B. Li, Y.-L. Chen, Y. Li, and Q. Gong, *Phys. Rev. A* **85**, 031805(R) (2012).
- <sup>34</sup>See Supplemental Material at <http://link.aps.org/supplemental/10.1103/PhysRevB.86.045309> for a magnified view of the field distributions.